HHS Public Access

Author manuscript

Stem Cells. Author manuscript; available in PMC 2017 January 26.

Published in final edited form as:

Stem Cells. 2016 June ; 34(6): 1615–1625. doi:10.1002/stem.2305.

The Antiaging Gene *Klotho* Regulates Proliferation and Differentiation of Adipose-Derived Stem Cells

Jun Fan and **Zhongjie Sun**

Department of Physiology, College of Medicine, University of Oklahoma Health Sciences Center, Oklahoma City, Oklahoma, USA

Abstract

Klotho was originally discovered as an aging-suppressor gene. The purpose of this study was to investigate whether secreted Klotho (SKL) affects the proliferation and differentiation of adipose-derived stem cells (ADSCs). RT-PCR and Western blot analysis showed that short-form Klotho was expressed in mouse ADSCs. The *Klotho* gene mutation *KL*(−/−) significantly decreased proliferation of ADSCs and expression of pluripotent transcription factors (Nanog, Sox-2, and Oct-4) in mice. The adipogenic differentiation of ADSCs was also decreased in *KL*(−/−) mice. Incubation with Klotho-deficient medium decreased ADSC proliferation, pluripotent transcription factor levels, and adipogenic differentiation, which is similar to what was found in *KL*(−/−) mice. These results indicate that Klotho deficiency suppresses ADSC proliferation and differentiation. Interestingly, treatment with recombinant SKL protein rescued the Klotho deficiency-induced impairment in ADSC proliferation and adipogenic differentiation. SKL also regulated ADSCs' differentiation to other cell lineages (osteoblasts, myofibroblasts), indicating that SKL maintains stemness of ADSCs. It is intriguing that overexpression of SKL significantly increased PPAR-γ expression and lipid formation in ADSCs following adipogenic induction, indicating enhanced adipogenic differentiation. Overexpression of SKL inhibited expression of TGFβ1 and its downstream signaling mediator Smad2/3. This study demonstrates, for the first time, that SKL is essential to the maintenance of normal proliferation and differentiation in ADSCs. Klotho regulates adipogenic differentiation in ADSCs, likely via inhibition of TGFβ1 and activation of PPAR-γ.

Keywords

Adipose stem cell; Adipogenic differentiation; Osteogenic differentiation; Myofibroblastic differentiation; TGFβ1; Cell proliferation

Correspondence: Zhongjie Sun, M.D., Ph.D., F.A.H.A., The Robert & Mary Cade Laboratory, BMSB 662A, Box 26901, Department of Physiology, BMSB 662A, College of Medicine, University of Oklahoma Health Sciences Center (OUHSC), 940 S.L. Young Blvd., Oklahoma City, Oklahoma 73126-0901, USA. Telephone: 405-271-2226 x 56237; Fax: 405-271-3181; Zhongjie-sun@ouhsc.edu.

Author Contributions

Z.S.: developed the concepts and hypotheses designed the study and participated in writing the manuscript J.F.: conducted the experiments analyzed the data and participated in writing the manuscript.

Competing Financial Interests

The authors declare that they have no competing financial interests.

J. F. is currently affiliated with the Department of Tissue Engineering, School of Fundamental Sciences, China Medical University, Shenyang, China.

Introduction

Mesenchymal stem/stromal cells (MSCs) are multipotent cells capable of self-renewal and differentiation into tissue-specific cell types. Among the various sources of MSCs, adipose-derived stem cells (ADSCs) are abundant and easily obtained from subcutaneous adipose tissue via liposuction in the clinic [1]. ADSCs have been shown to possess multi-lineage potential, capable of differentiating into adipogenic, osteogenic, myogenic, and chondrogenic cells [2], and ADSC-based transplantation is a promising therapeutic approach for tissue regeneration and repair. Understanding the molecular mechanisms involved in ADSC proliferation and differentiation is therefore of paramount importance.

Pluripotency markers, such as Oct-4, Nanog, and Sox-2, play a significant role in the renewal and differentiation abilities of ADSCs [3]. ACSCs with overexpression of Oct-4 and Sox-2 in ADSCs show an enhanced ability to differentiate into adipocytes and osteoblasts relative to controls [4]. In human bone marrow stromal cells (BMSCs), increased Oct-4 and Nanog expression also promotes proliferation and differentiation potential [5]. Aging is associated with the reduction in self-renewal capacity and differentiation potential of MSCs, and old BMSCs demonstrate lower levels of Oct-4 compared with young BMSCs and do not express Sox-2 and Nanog [6]. Aging cells also enlarge, become more granular, and proliferate slowly. Several types of MSCs show lower cell yields and impaired adipogenesis with age [7].

Klotho was originally identified as an aging-suppressor gene and is mainly expressed in the kidney and the brain choroid plexus. In mice, overexpression of Klotho extends life span [8], while disruption of the *Klotho* gene results in accelerated aging and shortened lifespan [9]. There are three forms of Klotho: membrane Klotho, soluble Klotho, and secreted Klotho (SKL). Soluble Klotho is generated by shedding the extracellular domain of the transmembrane protein, whereas SKL can be generated by alternative RNA splicing [9]. SKL protein is then released from the cell into the extracellular space and emerges in blood, urine, and cerebrospinal fluid [10, 11]. SKL functions as an endocrine factor and targets distant organs, and it regulates the activity of ion channels and transporters on the cell surface [12–14]. Both membrane and secreted forms of the Klotho protein were detected in the 3T3-L1 cell line [15]. During adipose differentiation in 3T3-L1 adipocytes, the membrane form of Klotho gradually increases in abundance, but the secreted form is not altered [15]. In vitro studies showed that overexpression of Klotho in the 3T3-L1 cell line facilitated the differentiation of preadipocytes into mature adipocytes [16]. However, whether Klotho affects the proliferation and differentiation of ADSCs is unclear and is the subject of investigation in this study.

TGF-β1, the most abundant isoform of the TGF-β family, plays an important role in cell growth, differentiation, and development. It induces chondrogenic or smooth muscle cell differentiation of MSCs in vitro and also inhibits adipogenic differentiation of MSCs [17]. TGF-β1 is known to inhibit adipose differentiation of preadipocyte cell lines and ADSCs [18] and also blocks adipogenesis in vivo [19]. It was previously reported that Klotho inhibited TGF-β1 and suppresses the epithelial-to-mesenchymal transition in A549 cells

[12]. It is not clear, however, whether SKL regulates TGF-β1 signaling in the adipogenic differentiation of ADSCs.

The objective of this study is to investigate whether SKL plays a role in the regulation of proliferation and adipogenic differentiation in ADSCs.

Materials and Methods

Isolating ADSCs for Cultures

Adipose tissues were obtained from inguinal subcutaneous fat from *KL*(−/−) mice in a 129Sv background and wild type (WT) littermate 129Sv mice (4–5 weeks). An equal volume of 0.1% type I collagenase was used to digest the samples in a 37°C water bath with shaking for 1 hour. The digestion reaction was terminated with DMEM/F12 (Thermo Fisher Scientific, Grand Island, NY, http://www.thermofisher.com) containing 10% fetal bovine serum (FBS) with 1% penicillin-streptomycin. The digestion product was then centrifuged at 800*g* for 5 minutes. The resultant supernatant was discarded, and the corresponding precipitate was suspended with DMEM/F12 and centrifuged after filtration. The pellet was suspended in DMEM/F12 containing 10% FBS and 1% penicillin-streptomycin to obtain a homogeneous suspension. Finally, the suspension was transferred to a flask and cultured at 37°C with 5% CO_2 in a humidified atmosphere. The culture medium was changed every 3 days, and the cells were passaged after 80%–90% confluence. The third-passage cells were used for flow cytometry. Human adipose-derived stem cells (hADSCs, Lonza, Allendale, NJ, http://www.lonza.com/) and mouse bone marrow-derived stem cells (mMSCs, Thermo Fisher Scientific) were also cultured under the same conditions.

Flow Cytometry

The isolated ADSC phenotype was confirmed by assessing native markers (CD34 and CD45) and positive markers (CD44 and CD105) using flow cytometry as described before [20]. Third-passage ADSCs underwent digestion with 0.25% trypsin-EDTA and centrifugation at 800*g* for 5 minutes. The resultant supernatant was discarded, and the cell pellet was washed with PBS. A homogeneous cell suspension with a cell density of 1×10^6/ml was obtained using a small volume of PBS. Cell suspension aliquots were then transferred to individual EP tubes (200 μl/tube). CD45, CD44, CD105 (BD Biosciences Pharmingen, San Diego, CA, http://www.bdbiosciences.com), and CD34 (Abcam, Cambridge, MA, http://www.abcam.com) were added to different individual tubes, and aliquots without antibodies served as the negative controls. All samples were kept away from light for 30 minutes and then washed with PBS to remove unbound antibodies. After centrifugation at 800*g* for 5 minutes, 500 μl PBS was added to each tube for fluorescence-activated cell sorting analysis.

Cell Proliferation and Colony Formation

ADSCs were isolated from WT and *KL*(−/−) mice. The cell proliferation rate was monitored at different time points (days 1, 3, 5, 7, and 9) using the MTT assay. For the colony-formation assay, ADSCs (1×10^4) were seeded in a 10-cm dish and incubated at 37°C in a 5% CO_2 atmosphere. Non-adherent cells were removed, and the adherent cells were cultured

in maintenance medium after 24 hours. On day 14, ADSCs were fixed with 4% paraformaldehyde and stained with 0.5% crystal violet (Sigma-Aldrich, St. Louis, MO, http://www.sigmaaldrich.com) in methanol for 10 minutes at room temperature before counting the cell colonies. All experiments were independently repeated at least three times.

Multipotential Induction of ADSCs and mMSCs

Adipogenic differentiation was induced in DMEM/F12 (Thermo Fisher Scientific) supplemented with 10% FBS, dexamethasone (1 μM), insulin (10 μM), indomethacin (200 μM), and 3-isobutyl-1-methylxanthine (0.5 μM, Sigma-Aldrich). Oil Red O staining was performed to visualize lipid droplets, as described previously [21]. After microscopic study, quantification of lipid accumulation was measured by an Oil Red O staining extraction assay. Isopropanol (100%) was added to each well and gently mixed, the extract transferred to a 96-well plate, and the absorbance recorded at 510 nm. For osteogenic differentiation, confluent ADSCs were cultured and treated with 0.1 mM dexamethasone (Sigma-Aldrich), 10 mM β-glycerophosphate (Sigma-Aldrich), and 50 μM ascorbic acid (Sigma-Aldrich). The osteoblast phenotype was indicated by alkaline phosphatase (ALP) determination, an early marker of osteogenic differentiation. For ALP staining, cells were rinsed with PBS, fixed with 4% paraformaldehyde for 2 minutes and stained with an ALP detection kit (EMD Millipore, Billerica, MA, http://www.emdmillipore.com). The ALP activity in the samples was measured using a colorimetric SensoLyte pNPP Alkaline Phosphatase Assay Kit (AnaSpec, Fremont, CA, http://www.anaspec.com/) according to the manufacturer's recommendation. Alizarin Red S staining was performed to detect matrix mineralization deposition at the late stage of bone formation. To induce differentiation of ADSCs into myofibroblasts, ADSCs were treated with 2 ng/mL TGF-β1 (R&D Systems, Minneapolis, MN, http://www.rndsystems.com) for 4 days. TGF-β1-induced differentiation of ADSCs into myofibroblasts was confirmed by examining α-SMA (1:200, Abcam) expression by immunohistochemistry.

Plasmid Construction

The pAAV-MCS plasmid vector was purchased from Stratagene (Stratagene, La Jolla, CA, www.stratagene.com). The plasmid pAAV-mKlotho was constructed by inserting mouse SKL cDNA into the EcoRI and Xba I sites of the pAAV-MCS expression vector. Plasmids were amplified in *Escherichia coli* DH5α cells, extracted by the alkaline lysis method, and purified using a Qiagen Endo-free Plasmid Maxi Kit (Qiagen, Valencia, CA, http://www.qiagen.com). The quantity and quality of the purified plasmid DNA were assessed by determining the absorbance at 260 and 280 nm and also by electrophoresis in agarose gels. The plasmids were dissolved in TE buffer before use.

Purification of Recombinant Mouse SKL

A 6xHis tag was inserted into the pAAV-mSKL plasmid for construction of the pAAV-Skl-6xHis plasmid, which was transfected into 293 cells using Lipofectamine Plus 2000. The culture medium was collected after 3 days transfection, and the recombinant His-tagged, SKL was purified with the His GraviTrap (GE, Healthcare, Piscataway, NJ, http://www.gehealthcare.com). The purity of the recombinant SKL (rSKL) proteins was confirmed

by sodium dodecylsulfate polyacrylamide gel electrophoresis (SDS-PAGE) stained with Coomassie blue and Western blotting antibodies.

Generation of Klotho-Deficient Serum

The direct immunoprecipitation (IP) method (Pierce Direct IP Kit, Pierce Biotechnology, Rockford, IL, http://www.thermoscientific.com/pierce) was used to remove SKL from FBS. Briefly, the coupling of Klotho antibody (R&D Systems) to AminoLink Plus Coupling Resin was performed according the manufacturer's manual, and control medium was generated by the coupling of IgG to the AminoLink Plus Coupling Resin. Serum (450 μl, Sigma) was added to the Klotho antibody-coupled resin in the spin column and incubated with shaking for 24 hours at 4°C. The column was then centrifuged and the serum collected. IP Lysis/ Wash Buffer (300 μl) was then added to the spin column, which was centrifuged. The spin column was then placed into a new collection tube, elution buffer added, and the spin column again centrifuged. After elution, undepleted serum was again added to the column and the procedure repeated as described above. Any residual Klotho protein was then identified by Western blot.

Western Blotting

The cells were washed twice with PBS and lysed. The total protein levels were measured using a BCA protein assay kit (Thermo Fisher Scientific). An equal amount of protein was loaded on a 4%–20% gradient SDS-PAGE gel, and the protein was transferred onto nitrocellulose filters after separation in the gel. Blots were blocked in 5% BSA in TBST for 1 hour at room temperature, and the membranes were then incubated with a primary antibody overnight at 4°C. The primary antibodies used were Klotho (1:300, R&D Systems), mouse anti-Oct-4 (1:1,000, EMD Millipore), rabbit anti-Sox-2 (1:1,000, Abcam), rabbit anti-Nanog (1:1,000, Abcam), anti-PPAR-γ (1:1,000, Cell Signaling, Danvers, MA, http://www.cellsignal.com), rabbit anti-TGF-β1(1:1,000, Santa Cruz Biotechnology, Inc., Dallas, Texas, http://www.scbt.com), rabbit anti-phospho-Smad2/3 (1:1,000, Cell Signaling), rabbit anti-Smad2/3 (1:1,000, Cell Signaling), rabbit anti-α-SMA (1:500, Abcam) and mouse anti-β-actin (1:10,000, Abcam). The membranes were incubated with HRP-conjugated secondary anti-goat, anti-mouse, or anti-rabbit antibodies (diluted in the range 1:2,000 to 1:5,000) for 1 hour at room temperature. Proteins were visualized by ECL using ChemDoc XRS with Quantity One Software (BioRad, Hercules, CA, http://www.bio-rad.com). Blots were repeated at least three times for every condition. To quantify and compare the levels of proteins, the density of each band was measured by densitometry.

ADSC Transfection

Subconfluent ADSCs were washed with PBS and incubated in trypsin/EDTA, PBS, and collagenase. The cells were resuspended and pelleted at 800*g* for 5 minutes and then resuspended in Opti-MEM I Reduced Serum Medium (Thermo Fisher Scientific). Five hundred microliters of cell suspension was transferred to a 0.4-cm electroporation cuvette (Bio-Rad), and 50 μg of each of the indicated plasmids were added. Empty vector (pcDNA3) was used to normalize the total DNA added in all experiments. The cells were electroporated using a Gene Pulser XceII instrument (Bio-Rad) at 0.18 kV and 950 μF, and the cells were allowed to recover for 10 minutes at room temperature. Equivalent amounts of cell

suspension and fresh medium were added together and plated according to the intended experiment.

RNA Isolation and RT-PCR

Total RNA was purified from mouse kidney and ADSCs using TRIzol Reagent, followed by the Qiagen RNeasy Mini Kit. RNA (2 μg) was reverse-transcribed using SuperScript III Reverse Transcriptase with random hexamers in the presence of 10 μl dNTP for 1 hour at 50°C. Exons 4 and 5 of mouse *Klotho* cDNA (forward, 5′-GGGTGACTGGGTCAATCT-3′ and reverse, 5′-GCAAAGTAGCCACAAAGGC-3′) were targeted, which generated a 339-bp PCR product for mouse *Klotho*.

PCR reactions (20 μl total volume) contained 1 μl of the above cDNA, 0.2 μM of the appropriate oligonucleotide primer pair, and Taq 2 × mix (New England Biolabs, Beverly, MA, http://international.neb.com). PCR amplification conditions were as follows: 95°C for 5 minutes followed by 30 cycles of 95°C for 1 minute, the optimized annealing temperature for each primer pair for 1 minute, and 68°C for 1 minute. The PCR products were separated on 1.5% agarose gels and stained with ethidium bromide. The bands were visualized using a ChemiDoc System Imager (Bio-Rad) and quantified using Image J software (NIH, Bethesda, Maryland, http://imagej.nih.gov).

Statistical Analysis

All the data were analyzed by one-way analysis of variance (ANOVA). The unpaired *t* test was used for comparisons between two groups. Significance was set at a 95% confidence limit.

Results

Klotho Deficiency Decreased Adipogenesis in Mice

To assess the effect of Klotho deficiency on adipogenesis, we used mice with *Klotho* gene deletion, *KL*(−/−) [10]. ADSCs were isolated from the inguinal adipose tissue of WT and *KL*(−/−) mice, cultured, and identified by flow cytometry using CD markers [20]. Expression of CD34 and CD45 was negative, while CD44 and CD105 were highly expressed in isolated cells (Supporting Information Fig. S1). The multiple differentiation capacity (adipogenic, osteogenic, and myofibroblastic differentiation) of the ADSCs were also identified (Supporting Information Fig. S2). The results confirmed that the isolated cells were ADSCs [20, 22].

Western blot analysis indicated that only short-form Klotho protein (SKL, 65 kDa) was expressed in ADSCs in WT mice (Fig. 1A), but the long-form Klotho protein (130 kDa) was not detectable (not shown). RT-PCR analysis showed that Klotho mRNA was expressed in ADSCs in WT mice, although weakly (Fig. 1B). SKL mRNA and protein expression were barely detectable in ADSCs in *KL*(−/−) mice (Fig. 1A, 1B), suggesting efficient deletion of the *Klotho* gene.

To examine the effect of Klotho on the adipose tissue mass, we measured the weight of subcutaneous adipose tissue. The adipose tissue weight was decreased significantly in *KL*(−/

−) mice versus WT mice (Fig. 1C). Some of the *KL*(−/−) mice did not have adipose tissue, which was replaced by fibrous tissue. Morphologically, the isolated ADSCs of the WT mice were in a spindle (healthy) shape, whereas ADSCs of *KL*(−/−) mice had lost the spindle shape and became enlarged and flattened (Fig. 1D), a sign of cell senescence.

Klotho Deficiency Decreased Cell Proliferation and Pluripotent Transcription Factor Expression in ADSCs

A cell proliferation assay (MTT) showed that cell proliferation was decreased in ADSCs of *KL*(−/−) mice versus WT mice (Fig. 2A). Colony-forming unit analysis revealed a decrease in colony formation in ADSCs of *KL*(−/−) mice versus WT mice (Fig. 2B), suggesting a decrease in ADSC proliferation.

Western blot analysis showed that protein expression of the pluripotency-associated transcription factors Nanog, Sox-2, and Oct-4 was decreased in ADSCs of *KL*(−/−) mice compared with the ADSCs of WT mice (Fig. 2C).

This finding indicated that Klotho deficiency suppressed ADSC proliferation potential.

Klotho Deficiency Attenuated Adipogenic Differentiation in ADSCs

To explore whether Klotho affects adipogenic differentiation in ADSCs, we used adipogenic induction medium to induce differentiation in cultured ADSCs from *KL*(−/−) and WT mice. The cells were stained with Oil Red O stain following incubation with the induction medium for 7 days. The lipid-positive cells were counted using NIH Image J software, and isopropanol elution was also used to quantify the accumulated lipid. The percentage of lipid-positive cells was decreased significantly in ADSCs isolated from *KL*(−/−) mice versus WT mice (Fig. 3A, 3B). Lipid accumulation (Oil Red O staining) was also attenuated in ADSCs in *KL*(−/−) mice compared with WT mice (Fig. 3C). These results suggest that Klotho deficiency inhibited adipogenic differentiation.

PPAR-γ is a marker of adipocyte differentiation, and its expression in the ADSCs of *KL*(−/−) mice was decreased remarkably compared with that of WT mice following adipogenic induction (Fig. 3D). This result suggests that Klotho deficiency impairs adipogenic differentiation in ADSCs.

rSKL Protein Rescued the Klotho Deficiency-Induced Decrease in Cell Proliferation and Pluripotent Transcription Factor Expression in ADSCs

SKL is a secreted protein in serum. Therefore, we investigated whether removal of SKL from serum affects pluripotent transcription factor expression and cell proliferation. Klotho was removed from the serum using the direct IP method (Supporting Information Fig. S3). The recombinant mouse SKL protein was generated from HEK293 cells with overexpression of SKL (Supporting Information Fig. S4). Treatment with Klotho-deficient serum for 48 hours changed the ADSCs from spindle shapes (healthy) to flattened shapes (unhealthy), and rSKL protein rescued these morphological changes (Supporting Information Fig. S5).

MTT analysis showed that cell proliferation of ADSCs decreased following treatment with Klotho-deficient serum, which was rescued by rSKL (Fig. 4A). The expression of Oct-4 and

Sox-2 decreased significantly in ADSCs treated with Klotho-deficient serum, which was reversed by treatment with recombinant Klotho protein (Fig. 4B–4D). Nanog expression was slightly, but not significantly, decreased by Klotho-deficient serum, and recombinant Klotho protein increased its expression (Fig. 4B, 4E).

rSKL Rescued the Klotho Deficiency-Induced Decrease in Adipogenic Differentiation in ADSCs

Since Klotho deficiency in serum affected cell proliferation and pluripotent transcription factor expression, we further assessed whether Klotho deficiency affects adipogenic differentiation in mouse ADSCs. The ADSCs were incubated in Klotho-deficient serum with or without SKL, treated with adipogenic induction medium for 7 days, and stained with Oil Red O stain (Fig. 5A). The results indicated that adipogenic differentiation was decreased by Klotho deficiency, and this effect was abolished by rSKL (Fig. 5A–5C). Western blot analysis showed that PPAR-γ, an adipogenic differentiation marker, was attenuated by Klotho deficiency, which could be rescued by rSKL (Fig. 5D).

Klotho deficiency also decreased adipogenic differentiation in hADSCs which was rescused by rSKL (Supporting Information Fig. S6). We also examined the effect of SKL on adipogenesis in another type of stem cells. mMSCs were incubated with Klotho-deficient serum with or without addition of rSKL, then induced by adipogenic differentiation medium for 7 days. The results demonstrated that rSK rescued the Klotho deficiency-induced impairment in adipogenic differentiation in mMSCs (Supporting Information Fig. S7).

Overexpression of SKL Inhibited TGFβ1 Signaling in ADSCs

TGFβ1 inhibits adipogenic differentiation [18, 23]. To explore the molecular mechanism of the effects of SKL on adipogenic differentiation in ADSCs isolated from WT mice (normal), we assessed TGF-β1 and the downstream signaling level of p-Smad2/3 in ADSCs with overexpression of SKL. Overexpression of SKL was achieved by transfection of ADSCs with pAAV-mSKL plasmid DNA (driven by the cytomegalovirus promoter). Morphologically, overexpression of SKL changed the ADSCs to a more spindle-like, healthy shape (Fig. 6A). As shown in Figure 6B, transfection with pAAV-mSKL for 48 hours significantly increased SKL protein levels in ADSCs compared with the control group and the green fluorescence protein GFP (pAAV-GFP) group. SKL gene transfer resulted in SKL (65 kDa) protein expression (Fig. 6B, 6C), but didn't induce membrane Klotho (130 kDa) expression (Supporting Information Fig. S8).

Overexpression of SKL significantly decreased TGF-β1 expression in ADSCs compared with the control groups (Fig. 6B, 6D). Consistent with the role of p-Samd2/3 as a mediator of TGFβ signaling, overexpression of SKL also decreased the p-Samd2/3 level in ADSCs (Fig. 6B, 6E). Overexpression of SKL, however, did not alter the expression of Nanog, Sox-2, and Oct-4 in ADSCs (Supporting Information Fig. S9).

Overexpression of SKL Facilitated Adipogenic Differentiation in ADSCs

To investigate the effect of SKL overexpression on adipogenic differentiation in ADSCs, we assessed lipid formation in ADSCs transfected with plasmid DNA pAAV-mSKL. After 7

days of incubation in adipogenic induction medium, ADSCs were stained with Oil Red O stain (Fig. 7A). The percentage of lipid-positive ADSCs (Fig. 7B) and lipid accumulation (Fig. 7C) were both increased significantly by overexpression of SKL, suggesting that SKL enhances adipogenic differentiation. Western blot analysis revealed that overexpression of SKL increased expression of PPAR-γ, an adipogenesis marker, in ADSCs (Fig. 7D). These results demonstrate, for the first time, that SKL facilitates adipogenic differentiation in ADSCs.

rSKL Protein Reversed the Inhibitory Effect of TGFβ1 on Adipogenic Differentiation in ADSCs

To further investigate the biological function of SKL on TGFβ1 signaling in the process of adipogenic differentiation of ADSCs, these cells were treated with rSKL, TGFβ1, or rSKL plus TGFβ1 for 2 days. ADSCs were then incubated with adipogenic induction medium for 7 days before staining with Oil Red O stain. The results showed that treatment with TGF-β1 inhibited adipogenic differentiation (Supporting Information Fig. S10A, 10B). The inhibitory action of TGF-β1 on adipogenic differentiation of ADSCs was attenuated by rSKL (Supporting Information Fig. S10A–10C). Protein expression of PPAR-γ, a marker of adipogenic differentiation, was decreased by TGFβ1, which was abolished by rSKL (Supporting Information Fig. S10D). Therefore, rSKL antagonizes the inhibitory action of TGFβ1 in ADSC differentiation.

rSKL Protein Inhibits TGFβ1 Signaling in ADSCs

To further assess the effect of SKL on TGFβ1 signaling in ADSCs, we treated ADSCs with different concentrations of rSKL for 48 hours. Western blot analysis showed that rSKL dose-dependently decreased TGFβ1 expression in ADSCs (Supporting Information Fig. S11A, 11B). The TGFβ1 signaling mediator p-Smad2/3 was also attenuated with increased concentrations of rSKL (Supporting Information Fig. S11A, 11C). Therefore, rSKL inhibited TGFβ1 signaling in ADSCs.

SKL did not affect protein levels of Oct-4, Nanog, and Sox-2 significantly in ADSCs (Supporting Information Fig. S12), which was consistent with the result for SKL overexpression (Supporting Information Fig. S6).

SKL Mediated the Stemness of ADSCs

To explore whether SKL regulates ADSCs' differentiation to other cell lineages, ADSCs were undergone with osteogenic and myofibroblastic induction in Klotho-deficient serum with or without addition of rSKL. The results showed that osteogenic and myofibroblastic differentiation capacities were decreased due to Klotho deficiency, which was reversed by addition of rSKL (Supporting Information Figs. S13, S14). Therefore, SKL may mediate the stemness of ADSCs.

Discussion

Klotho was originally identified as an aging-suppressor gene and is implicated in a variety of biological processes [9, 10, 24]. Klotho is primarily expressed in kidneys and the brain

choroid plexus [9]. In this study, we found that Klotho was expressed in mouse ADSCs, as evidenced by expression of Klotho mRNA and protein (Fig. 1A, 1B). The major Klotho protein in mouse ADSCs is SKL, with an apparent molecular mass of 65 kDa (Fig. 1A). *Klotho* gene mutation decreased ADSC proliferation, adipogenesis, and differentiation in mice (Figs. 1–3), suggesting, for the first time, that Klotho is essential to the maintenance of normal proliferation and differentiation in ADSCs. On the other hand, overexpression of the *Klotho* gene or administration of the Klotho protein enhanced ADSC proliferation and promoted adipogenic differentiation in ADSCs (Figs. 4–7). This study provides new and important evidence that SKL regulates ADSC proliferation and differentiation.

ADSCs have self-renewal and multiple differentiation potentials that are critical for tissue regeneration and repair and are particularly promising for regenerative therapies [25, 26]. However, their therapeutic potential may be limited due to cell senescence [27]. Stem cell dysfunction or depletion might contribute to aging [28], and in recent years, Klotho, as an aging-suppressor gene, has attracted much attention [9]. Overexpression of the *Klotho* gene extends lifespan, while its mutation leads to rapid aging and early death [29]. The SKL level declines with age [9, 30, 31], while the number of senescent and dysfunctional stem cells increases with age [32–34]. Aging impairs stem cell proliferation [35–37], and stem cell proliferation and differentiation decrease in an age-dependent manner [37–39]. The number of stem cells is decreased while the percentage of the senescent progenitor cells is increased in tissues and organs in *KL*(−/−) mice [28]. Genetic ablation of *Klotho* in mice results in a significant decrease in the hematopoietic stem cell pool size in bone marrow and impaired hematopoietic stem cell homing in vivo [40]. It remains unclear, however, whether the impairment in stem cells is attributable directly to Klotho deficiency or is secondary to hyperphosphetemia due to Klotho deficiency. In this study, we found that cell proliferation was decreased in ADSCs isolated from *KL*(−/−) mice (Fig. 2). In addition, Klotho deficiency impaired ADSC health, as evidenced by an enlarged and flattened cell shape in *KL*(−/−) mice versus the healthy spindle shape in WT mice (Fig. 1). Similarly, incubation with Klotho-deficient medium decreased the proliferation of ADSCs isolated from WT mice (Fig. 4) and resulted in a change of cell morphology to an enlarged and flattened shape (Supporting Information Fig. S4), a sign of MSC senescence. These changes were rescued by adding rSKL protein (Supporting Information Fig. S4). Therefore, this study demonstrates that SKL directly regulates and maintains normal cell viability and proliferation of ADSCs.

The self-renewal capacity of embryonic stem cells is regulated by core pluripotent transcription factors, such as Oct-4, Sox-2, and Nanog [41], which also control ADSC differentiation abilities [42]. Overexpression of these transcription factors enhances the capacity of ADSCs to differentiate toward adipogenesis or osteogenesis [4]. In this study, we found that expression of Nanog, Sox-2, and Oct-4 was decreased in ADSCs in *KL*(−/−) mice (Fig. 2) and in ADSCs cultured with Klotho-deficient medium (Fig. 4). The downregulation of these transcription factors contributed to Klotho deficiency-induced impairment in adipogenic differentiation (Figs. 3 and 5). Therefore, SKL is an important factor that maintains the stemness of ADSCs, as SKL deficiency downregulates pluripotent transcription factor expression and impairs adipogenesis in ADSCs. Interestingly, rSKL rescued the downregulation of Nanog, Sox-2, and Oct-4 and normalized adipogenesis in

ADSCs cultured in Klotho-deficient medium (Figs. (4 and 5)). By contrast, overexpression of SKL or treatment with rSKL protein did not alter the expression of Oct-4, Nanog, and Sox-2 in ADSCs isolated from WT mice cultured in normal serum (Supporting Information Fig. S6), suggesting that excess Klotho does not affect these transcription factors in normal ADSCs. However, overexpression of SKL enhanced adipogenic differentiation (Fig. 7).

Overexpression of SKL or treatment with rSKL protein decreased TGFβ1 expression and its downstream Smad2/3 targets in ADSCs (Fig. 6, Supporting Information Fig. S8). Therefore, SKL inhibited TGFβ1 signaling in ADSCs. SKL binds to TGFBR2 and inhibits TGF-β1 binding to the cell surface receptors, thereby inhibiting TGF-β1 signaling [12]. TGF-β1 regulates the differentiation process in several types of cells, including muscle, bone, cartilage, and adipocytes [43]. TGFβ1 was reported to inhibit adipose differentiation in preadipocyte cell lines and ADSCs [18, 23]. In mice, transgenic overexpression of TGF-β1 in adipose tissue significantly reduced both white and brown adipose tissue in extent and exhibited prominent fibroplasia [19]. Once TGF-β signaling is activated, the TGF-β superfamily of growth factors signals via heteromeric complexes with type I (ALK) and type II receptors, recruiting downstream Smad proteins before translocating to the nucleus and acting as a transcription factor on target genes [44]. TGFβ1 inhibits adipogenesis through its downstream target, Smad3, in a mouse preadipocyte cell line and in human ADSCs [18, 43]. TGF-β–Smad3 signaling inhibits adipogenic differentiation primarily through functional repression of C/EBPβ and C/EBPδ, thus preventing their transcriptional activity at the promoters of key adipogenic markers such as PPARγ [45]. Indeed, Klotho has been shown to upregulate C/EBPβ expression [46]. Chihara et al. found that Klotho also induced C/EBPα and PPARγ mRNA expression and promoted adipocyte differentiation [16]. PPARγ is known to play an important role in adipogenic differentiation. Therefore, SKL may enhance adipogenic differentiation in ADSCs by inhibition of TGFβ1 signaling, leading to upregulation of PPARγ.

In summary, this study provides the first evidence that SKL is expressed in ADSCs. It is new and interesting that SKL deficiency impairs ADSC proliferation and adipogenic, osteoblastic and myofibroblastic differentiation which were rescued by addition of rSKL. Therefore, SKL is essential to the maintenance of stemness of ADSCs. SKL promotes adipogenic differentiation in ADSCs by inhibiting TGFβ1 signaling and upregulating PPARγ.

Supplementary Material

Refer to Web version on PubMed Central for supplementary material.

Acknowledgments

This work was supported by NIH R01 grants HL118558, DK093403, HL116863, HL122166, HL105302, HL102074, and AG049780. This publication was made possible by NIH Grant Number 9P20GM104934-06 from the COBRE Program of the National Institute of General Medical Sciences.

References

1. Doi K, Tanaka S, Iida H, et al. Stromal vascular fraction isolated from lipo-aspirates using an automated processing system: Bench and bed analysis. J Tissue Eng Regen Med. 2013; 7:864–870. [PubMed: 22438241]
2. Su SJ, Yeh YT, Su SH, et al. Biochanin a promotes osteogenic but inhibits adipogenic differentiation: Evidence with primary adipose-derived stem cells. Evid Based Complement Alternat Med. 2013; 2013:846039. [PubMed: 23843885]
3. Baer PC, Griesche N, Luttmann W, et al. Human adipose-derived mesenchymal stem cells in vitro: Evaluation of an optimal expansion medium preserving stemness. Cytotherapy. 2010; 12:96–106. [PubMed: 19929458]
4. Han SM, Han SH, Coh YR, et al. Enhanced proliferation and differentiation of Oct4- and Sox2-overexpressing human adipose tissue mesenchymal stem cells. Exp Mol Med. 2014; 46:e101. [PubMed: 24946789]
5. Tsai CC, Su PF, Huang YF, et al. Oct4 and Nanog directly regulate Dnmt1 to maintain self-renewal and undifferentiated state in mesenchymal stem cells. Mol Cell. 2012; 47:169–182. [PubMed: 22795133]
6. Asumda FZ, Chase PB. Age-related changes in rat bone-marrow mesenchymal stem cell plasticity. BMC Cell Biol. 2011; 12:44. [PubMed: 21992089]
7. Beane OS, Fonseca VC, Cooper LL, et al. Impact of aging on the regenerative properties of bone marrow-, muscle-, and adipose-derived mesenchymal stem/stromal cells. PloS One. 2014; 9:e115963. [PubMed: 25541697]
8. Kurosu H, Yamamoto M, Clark JD, et al. Suppression of aging in mice by the hormone Klotho. Science. 2005; 309:1829–1833. [PubMed: 16123266]
9. Xu Y, Sun Z. Molecular basis of klotho: From gene to function in aging. Endocr Rev. 2015; 36:174–193. [PubMed: 25695404]
10. Kuro-o M, Matsumura Y, Aizawa H, et al. Mutation of the mouse klotho gene leads to a syndrome resembling ageing. Nature. 1997; 390:45–51. [PubMed: 9363890]
11. Yamamoto M, Clark JD, Pastor JV, et al. Regulation of oxidative stress by the anti-aging hormone klotho. J Biol Chem. 2005; 280:38029–38034. [PubMed: 16186101]
12. Doi S, Zou Y, Togao O, et al. Klotho inhibits transforming growth factor-beta1 (TGF-beta1) signaling and suppresses renal fibrosis and cancer metastasis in mice. J Biol Chem. 2011; 286:8655–8665. [PubMed: 21209102]
13. Cha SK, Hu MC, Kurosu H, et al. Regulation of renal outer medullary potassium channel and renal K(+) excretion by Klotho. Mol Pharm. 2009; 76:38–46.
14. Hu MC, Shi M, Zhang J, et al. Klotho: A novel phosphaturic substance acting as an autocrine enzyme in the renal proximal tubule. FASEB J. 2010; 24:3438–3450. [PubMed: 20466874]
15. Mizuno I, Takahashi Y, Okimura Y, et al. Upregulation of the klotho gene expression by thyroid hormone and during adipose differentiation in 3T3-L1 adipocytes. Life Sci. 2001; 68:2917–2923. [PubMed: 11411791]
16. Chihara Y, Rakugi H, Ishikawa K, et al. Klotho protein promotes adipocyte differentiation. Endocrinology. 2006; 147:3835–3842. [PubMed: 16709611]
17. Zhao L, Hantash BM. TGF-beta1 regulates differentiation of bone marrow mesenchymal stem cells. Vitam Horm. 2011; 87:127–141. [PubMed: 22127241]
18. Kim YJ, Hwang SJ, Bae YC, et al. MiR-21 regulates adipogenic differentiation through the modulation of TGF-beta signaling in mesenchymal stem cells derived from human adipose tissue. Stem Cells. 2009; 27:3093–3102. [PubMed: 19816956]
19. Clouthier DE, Comerford SA, Hammer RE. Hepatic fibrosis, glomerulosclerosis, and a lipodystrophy-like syndrome in PEPCK-TGF-beta1 transgenic mice. J Clin Invest. 1997; 100:2697–2713. [PubMed: 9389733]
20. Liu HY, Chiou JF, Wu AT, et al. The effect of diminished osteogenic signals on reduced osteoporosis recovery in aged mice and the potential therapeutic use of adipose-derived stem cells. Biomaterials. 2012; 33:6105–6112. [PubMed: 22698723]

21. Wang JQ, Fan J, Gao JH, et al. Comparison of in vivo adipogenic capabilities of two different extracellular matrix microparticle scaffolds. Plast Reconstr Surg. 2013; 131:174e–187e. [PubMed: 23271527]
22. Dominici M, Le Blanc K, Mueller I, et al. Minimal criteria for defining multipotent mesenchymal stromal cells. The International Society for Cellular Therapy position statement Cytotherapy. 2006; 8:315–317. [PubMed: 16923606]
23. Park JG, Lee DH, Moon YS, et al. Rever-sine increases the plasticity of lineage-committed preadipocytes to osteogenesis by inhibiting adipogenesis through induction of TGF-beta pathway in vitro. Biochem Biophys Res Commun. 2014; 446:30–36. [PubMed: 24548409]
24. Wang Y, Sun Z. Current understanding of klotho. Ageing Res Rev. 2009; 8:43–51. [PubMed: 19022406]
25. Sun Q, Zhang Z, Sun Z. The potential and challenges of using stem cells for cardiovascular repair and regeneration. Genes Dis. 2014; 1:113–119. [PubMed: 25642448]
26. Forcales SV. Potential of adipose-derived stem cells in muscular regenerative therapies. Front Aging Neurosci. 2015; 7:123. [PubMed: 26217219]
27. Mantovani C, Terenghi G, Magnaghi V. Senescence in adipose-derived stem cells and its implications in nerve regeneration. Neural Regen Res. 2014; 9:10–15. [PubMed: 25206738]
28. Liu H, Fergusson MM, Castilho RM, et al. Augmented Wnt signaling in a mammalian model of accelerated aging. Science. 2007; 317:803–806. [PubMed: 17690294]
29. Sun Z. Aging, arterial stiffness, and hypertension. Hypertension. 2015; 65:252–256. [PubMed: 25368028]
30. Yamazaki Y, Imura A, Urakawa I, et al. Establishment of sandwich ELISA for soluble alpha-Klotho measurement: Age-dependent change of soluble alpha-Klotho levels in healthy subjects. Biochem Biophys Res Commun. 2010; 398:513–518. [PubMed: 20599764]
31. Xiao NM, Zhang YM, Zheng Q, et al. Klotho is a serum factor related to human aging. Chin Med J (Engl). 2004; 117:742–747. [PubMed: 15161545]
32. Bennett JA, Singh KP, Unnisa Z, et al. Deficiency in aryl hydrocarbon receptor (AHR) expression throughout aging alters gene expression profiles in murine long-term hematopoietic stem cells. PLoS One. 2015; 10:e0133791. [PubMed: 26208102]
33. Chen L, Liu J, Tao X, et al. The role of Pin1 protein in aging of human tendon stem/progenitor cells. Biochem Biophys Res Commun. 2015; 464:487–492. [PubMed: 26150353]
34. Mendelsohn AR, Larrick J. Stem cell depletion by global disorganization of the H3K9me3 epigenetic marker in aging. Rejuvenation Res. 2015; 18:371–375. [PubMed: 26160351]
35. Brunauer R, Kennedy BK. Medicine. Progeria accelerates adult stem cell aging. Science. 2015; 348:1093–1094. [PubMed: 26045423]
36. Dulken B, Brunet A. Stem cell aging and sex: Are we missing something? Cell Stem Cell. 2015; 16:588–590. [PubMed: 26046758]
37. Snoeck HW. Can metabolic mechanisms of stem cell maintenance explain aging and the immortal germline? Cell Stem Cell. 2015; 16:582–584. [PubMed: 26046756]
38. Liu H, Xia X, Li B. Mesenchymal stem cell aging: Mechanisms and influences on skeletal and non-skeletal tissues. Exp Biol Med (Maywood). 2015; 240:1099–1106. [PubMed: 26088863]
39. Nurkovic JS, Volarevic V, Lako M, et al. Aging of stem and progenitor cells: Mechanisms, impact on the therapeutic potential and rejuvenation. Rejuvenation Res. 2015 [Epub ahead of print].
40. Vadakke Madathil S, Coe LM, Casu C, et al. Klotho deficiency disrupts hematopoietic stem cell development and erythropoiesis. Am J Pathol. 2014; 184:827–841. [PubMed: 24412515]
41. Kallas A, Pook M, Trei A, et al. Assessment of the potential of CDK2 inhibitor NU6140 to influence the expression of pluripotency markers NANOG, OCT4, and SOX2 in 2102Ep and H9 cells. Int J Cell Biol. 2014; 2014:280638. [PubMed: 25477962]
42. Yu J, Tu YK, Tang YB, et al. Stemness and transdifferentiation of adipose-derived stem cells using L-ascorbic acid 2-phosphate-induced cell sheet formation. Biomaterials. 2014; 35:3516–3526. [PubMed: 24462360]
43. Choy L, Skillington J, Derynck R. Roles of autocrine TGF-beta receptor and Smad signaling in adipocyte differentiation. J Cell Biol. 2000; 149:667–682. [PubMed: 10791980]

44. Nakao A, Imamura T, Souchelnytskyi S, et al. TGF-beta receptor-mediated signalling through Smad2, Smad3 and Smad4. EMBO J. 1997; 16:5353–5362. [PubMed: 9311995]

45. Choy L, Derynck R. Transforming growth factor-beta inhibits adipocyte differentiation by Smad3 interacting with CCAAT/enhancer-binding protein (C/EBP) and repressing C/EBP transactivation function. J Biol Chem. 2003; 278:9609–9619. [PubMed: 12524424]

46. Wolf I, Levanon-Cohen S, Bose S, et al. Klotho: A tumor suppressor and a modulator of the IGF-1 and FGF pathways in human breast cancer. Oncogene. 2008; 27:7094–7105. [PubMed: 18762812]

Significance Statement

Klotho was originally discovered as an aging-suppressor gene. This study investigated whether secreted Klotho (SKL) affects the proliferation and differentiation of adipose-derived stem cells (ADSCs). The results demonstrate, for the first time, that SKL is essential to the maintenance of normal proliferation and differentiation in ADSCs. Klotho regulates adipogenic differentiation in ADSCs, likely via inhibition of TGFβ1 and activation of PPAR-γ. The finding fundamentally advanced the field of ADSCs which may facilitate the development of stem cell therapy using ADSCs.

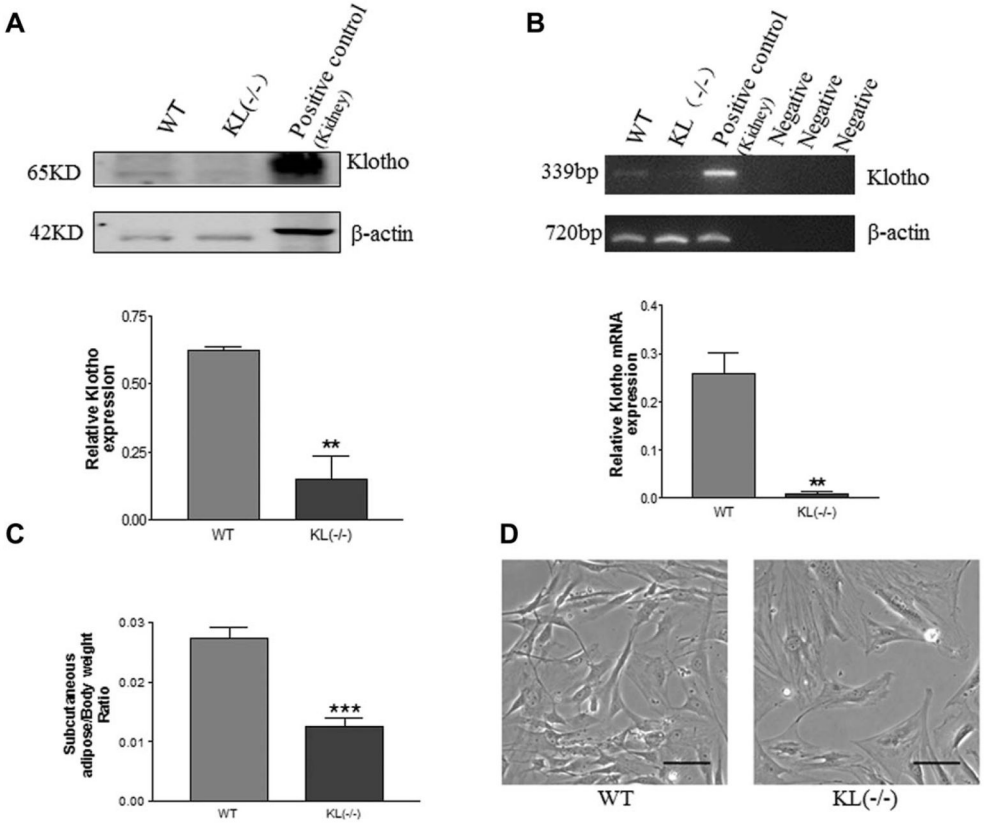

Figure 1.

Klotho deficiency decreased adipogenesis in mice. **(A)**: Western blot analysis of Klotho protein expression in adipose-derived stem cells (ADSCs) of WT and *KL*(−/−) mice. Mouse kidney lysates were used as a positive control for Klotho, which was expressed at 65 KD, while full-length Klotho protein (130 kDa) was not detectable. Results were normalized with β actin. **(B)**: RT-PCR analysis of Klotho mRNA in ADSCs of WT and *KL*(−/−) mice. Klotho mRNA in mouse kidney was used as the positive control. **(C)**: Subcutaneous adipose tissue weight in WT and *KL*(−/−) mice. **(D)**: Photomicrographs of ADSC morphology. ADSCs from WT mice had a spindle-like morphology (healthy), whereas ADSCs of *KL*(−/−) mice had a flattened shape (unhealthy). Scale bar, 100 μm. **, $p < .01$; ***, $p < .001$ versus the WT group. $n = 3$ independent experiments. Abbreviations: *KL*, WT, wild type.

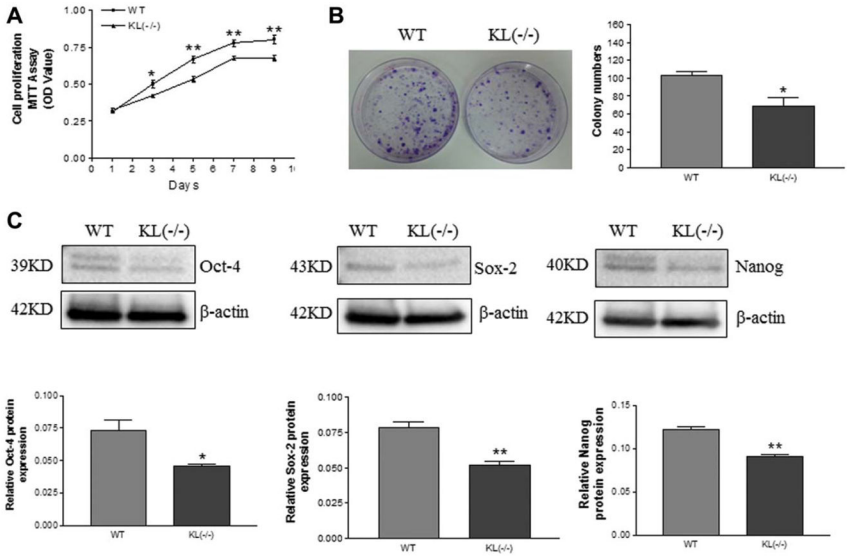

Figure 2.

Klotho deficiency decreased cell proliferation and pluripotent transcription factor expression in adipose-derived stem cells (ADSCs). **(A)**: MTT assay (optical densities) of the proliferation of ADSCs in WT and *KL*(−/−) mice over a period of 9 days. **(B)**: Colony formation of ADSCs cultured for 14 days. **(C)**: Western blot analysis of Nanog, Sox-2, and Oct-4 expression. Results were normalized with *β*-actin. *, $p < .05$; **, $p < .01$ versus the WT group. $n = 3$ independent experiments. Abbreviations: *KL*, WT, wild type.

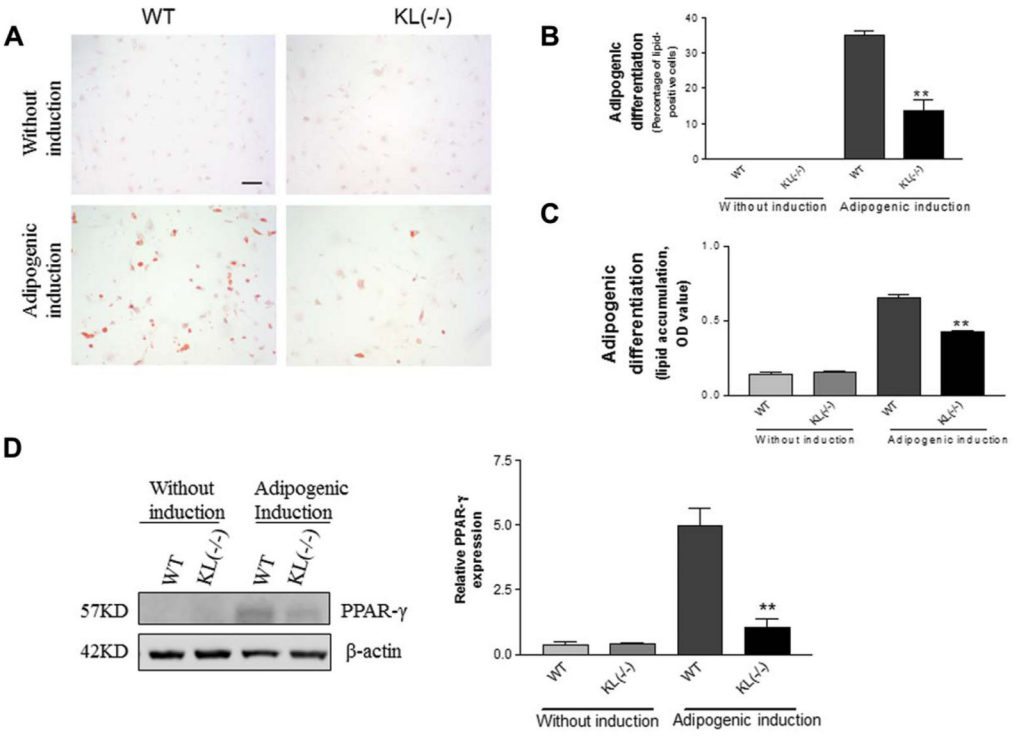

Figure 3.

Klotho deficiency attenuated adipogenic differentiation in adipose-derived stem cells (ADSCs). **(A)**: Lipid formation assessed by Oil Red O staining after 7 days of adipogenic induction. **(B)**: Quantification of lipid-positive cells (lipid vacuoles stained with Oil Red O stain) using NIH Image J software. **(C)**: Quantification of lipid accumulation (Oil Red O staining density). **(D)**: Western blot analysis of PPAR-γ expression in ADSCs. Results were normalized with β-actin. Scale bar =20 μm. **, $p < .01$ versus the WT group. $n = 3$ independent experiments.

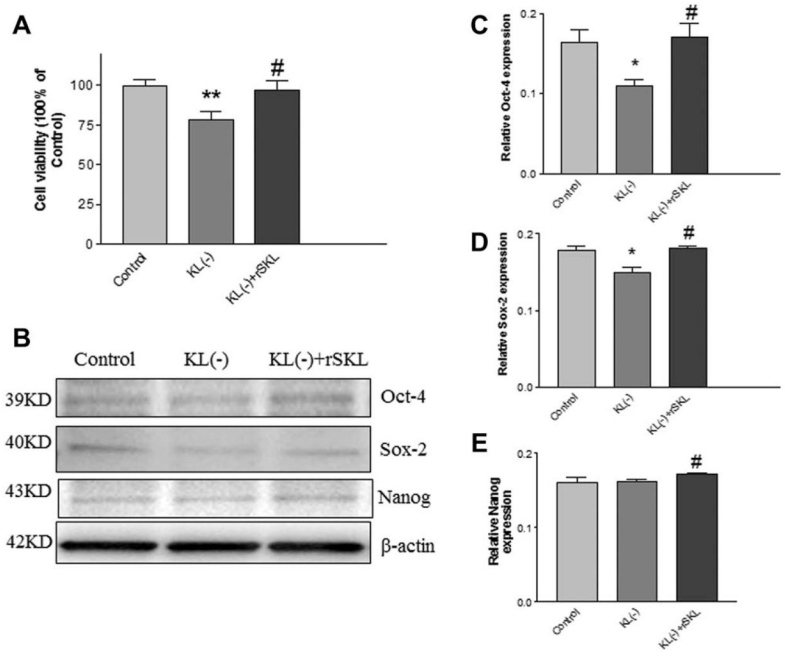

Figure 4.

rSKL protein rescued the Klotho deficiency-induced decrease in cell proliferation and pluripotent transcription factor expression in adipose-derived stem cells (ADSCs). **(A)**: MTT assay of the proliferation of ADSCs treated with Koltho-deficient serum and rSKL for 48 hours. **(B)**: Representative Western blot bands of Oct-4, Sox2, and Nanog. Quantification of Oct-4 **(C)**, Sox-2 **(D)**, and Nanog **(E)** expression. Results were standardized to β-actin. *, $p < .05$; **, $p < .01$ versus the control group; $^{\#}$, $p < .05$ versus the Klotho-deficient-serum group. $n = 3$ independent experiments. Abbreviations: *KL*, rSKL, recombinant SKL.

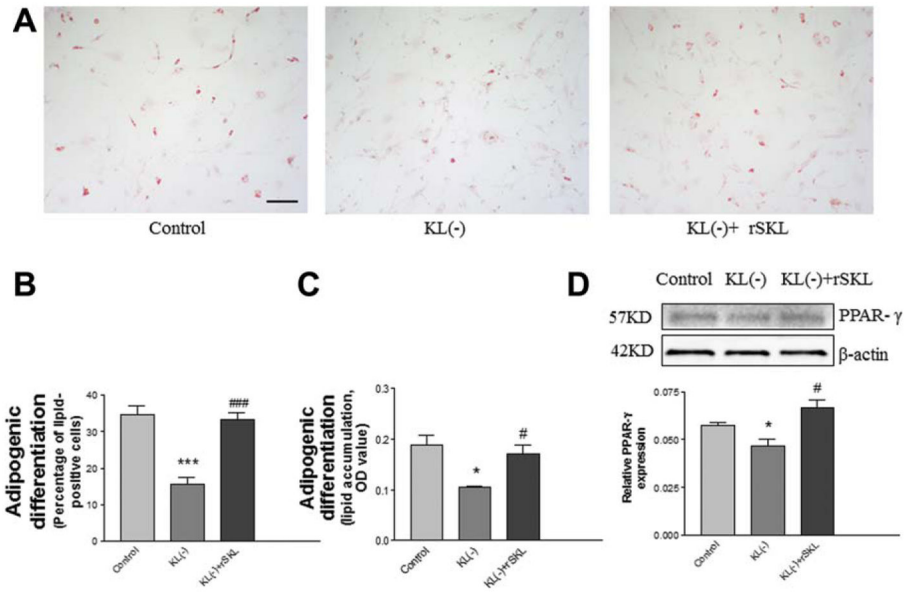

Figure 5.

rSKL rescued the Klotho deficiency-induced decrease in adipogenic differentiation in adipose-derived stem cells (ADSCs). **(A)**: Lipid formation assessed by Oil Red O staining after 7 days of adipogenic induction. **(B)**: Quantification of lipid-positive cells (lipid vacuoles stained with Oil Red O stain). Bar, 100 μm. **(C)**: Western blot analysis of PPAR-γ expression in ADSCs. Results were standardized to β-actin. *, $p < .05$; ***, $p < .001$ versus the control group; $^{\#}$, $p < .05$; $^{\#\#\#}$, $p < .001$ versus the KL(−) (Klotho-deficient) group. $n = 3$ independent experiments. Abbreviations: *KL*, rSKL, recombinant SKL.

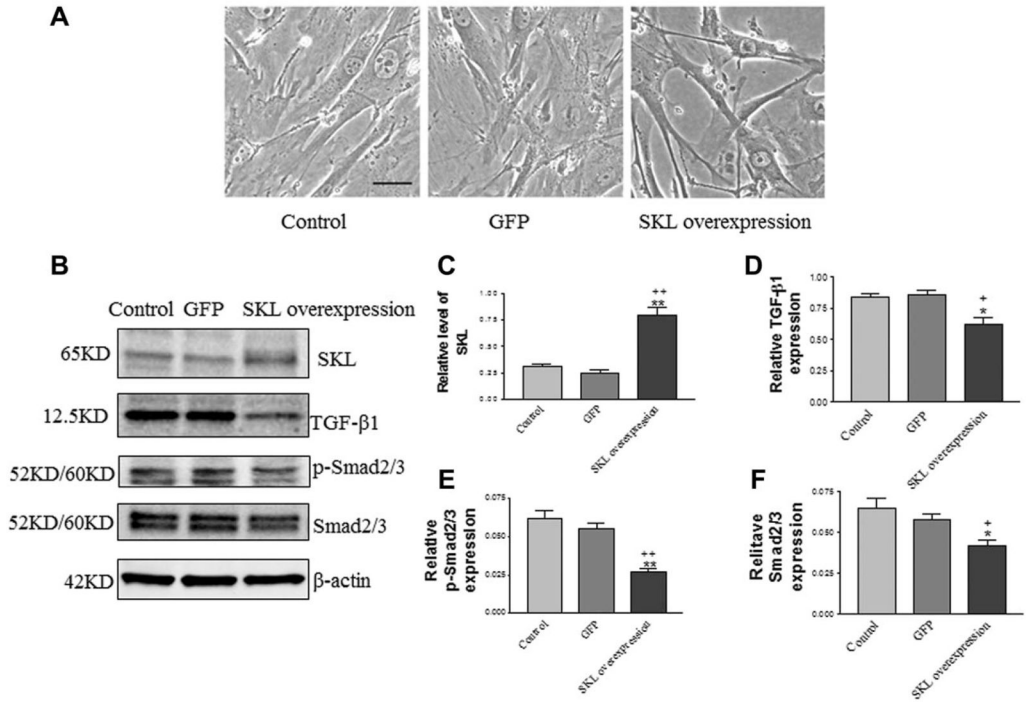

Figure 6.

Overexpression of SKL inhibited TGFβ1 signaling in adipose-derived stem cells (ADSCs). **(A)**: Morphology of ADSCs following overexpression of SKL. Cells had spindle-like shapes following overexpression of SKL. **(B)**: Western blot analysis of SKL, TGF-β1, p-Smad2/3, and Smad2/3 expression in ADSCs. Quantification of SKL **(C)**, TGF-β1 **(D)**, p-Smad2/3 **(E)**, and Smad2/3 **(F)** expression. Results were normalized with β-actin. Bar, 100 μm. *, p <.05 versus **, p <.001 versus the control group; $^{+}$, p <.05; $^{++}$, p <.01 versus the GFP group. n =3 independent experiments. Abbreviations: GFP, SKL, secreted Klotho.

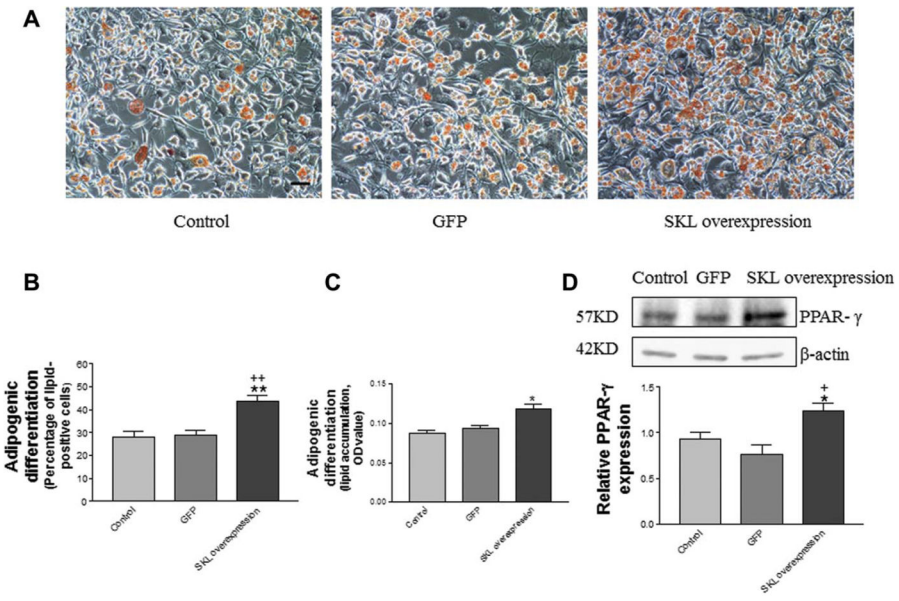

Figure 7.

Overexpression of SKL promoted adipogenic differentiation in adipose-derived stem cells (ADSCs). **(A)**: Lipid formation assessed by Oil Red O staining after 7 days of adipogenic induction. Scale bar, 100 μm. **(B)**: Quantification of lipid-positive cells (lipid vacuoles stained with Oil Red O stain). **(C)**: Quantification of lipid accumulation (Oil Red O staining density). **(D)**: Western blot analysis of PPAR-γ expression in ADSCs. Results were normalized with β-actin. *, $p < .05$; **, $p < .01$ versus the control group; $^{+}$, $p < .05$; $^{++}$, $p < .01$ versus the GFP group. Abbreviations: GFP, SKL, secreted Klotho.